Albero-Sancho, J.; Domínguez Torres, E.; Corma Canós, A.; García Gómez, H. (2017). Continuous flow photoassisted CO2 methanation. Sustainable Energy & Fuels. 1(6):1303-1307. doi:10.1039/c7se00246g

Journal Name

COMMUNICATION

Continuous Flow Photoassisted CO_2 Methanation

J. Albero[a], E. Dominguez[a], A. Corma[a] and H. García[a] *

Received 00th January 20xx,
Accepted 00th January 20xx

DOI: 10.1039/x0xx00000x

www.rsc.org/

Photoassisted CO_2 methanation using Ni-Al_2O_3/SiO_2 as photoresponsive catalysts has been carried out at 225 °C under continuous flow conditions achieving up to 3.5 % conversion of CO_2 with complete selectivity to CH_4 under 2327 W/m^2 irradiation for a contact time of 1.3 s. Apparent quantum yield of 0.11 was estimated for continuous flow process.

Photocatalytic CO_2 reduction is attracting considerable interest due to the urgent need to reduce drastically greenhouse gases emissions.[1, 2] In this context, sunlight can be employed to transform CO_2 gas into fuels, both in gas or liquid phase (CH_4, CO, HCOOH, etc.).[3] Due to the high rates that can be achieved and the overall high efficiency, one of the most promising reactions that has been proposed for industrial scale CO_2 transformation is the Sabatier reaction consisting in the catalytic formation of CH_4 by reaction of CO_2 and H_2 (Equation 1). To achieve low CO_2 emission footprint, H_2 has to be obtained from H_2O using renewable energy. Although the Sabatier methanation is an exothermic reaction, it requires temperatures between 250 - 400 °C depending on the catalysts type to achieve reaction rates adequate for large scale production.[4, 5] We and others have found that CO_2 methanation can be promoted at lower temperatures (about 250 °C or lower) photothermally using Ni-based catalysts[6, 7] as well as other transition metals (Co, Ru, ZnAl, etc.) supported in different semiconductors.[8, 9] This decrease in the reaction temperature and the use of solar light to promote CO_2 methanation makes the process environmentally more attractive by diminishing the dependency of this reaction on non-renewable energy resources. Thus, it is considered that due to the high conversion and selectivity that can be achieved in the methanation, the photoassisted CO_2 reduction can have some potential for the generation of solar fuels. H_2 should be available in the required high quantities from H_2O by electrolysis using renewable electricity.

$$CO_2 + 4\ H_2 \rightarrow CH_4 + 2\ H_2O \qquad \Delta H = -165\ \text{Kj/mol} \qquad (1)$$

Even though, there is by now a sufficiently large number of reports on the photoassisted methanation of CO_2 in batch mode,[8, 10-12] where a sealed reactor is charged with the required amounts of CO_2 and H_2 in contact with the photocatalyst that is irradiated through a transparent window until achieving high CO_2 conversions. In contrast, only few reports have studied this reaction in continuous flow operation,[13, 14] being much better suited for large scale processes, since it allows high production rates and easier automatization, resulting in optimal intensification of the process.[15] Ru based photocatalysts have been employed in continuous flow operation and high rates for CH_4 production obtained upon 10 Suns light intensity. This high light irradiation induced Ru nanoparticles to increase locally photocatalyst temperature (< 300 °C) in order to activate H_2 and initiate CO_2 hydrogentaion.[13]

On the other hand, one of the main characteristics of batch reactions is the accumulation of products which usually results in different selectivity due to the occurrence of consecutive reactions and the generation of secondary products.[16] However, continuous flow operation should provide high selectivity toward CH_4 production.

The above considerations show the interest of providing data about the continuous flow operation of the photoassisted CO_2 methanation and comparison with batch reaction. Aimed at filling this gap, the present study reports the continuous-flow photoassisted CO_2 methanation. The reaction has carried out in a tubular photoreactor in where the photoresponsive catalyst was deposited as a fixed bed exposed to irradiation with an optical fibre. In this communication, commercially available Ni-Al_2O_3/SiO_2 previously reported by us as one efficient photoresponsive material has been used, comparing the results obtained with those previously reported for the same material in batch conditions.[7, 17]

[a] *Instituto de Tecnología Química, Universitat Politècnica de València-Consejo superior de Investigaciones Científicas, Avenida de los Naranjos s/n, 46022 Valencia, Spain.*

Electronic Supplementary Information (ESI) available. See DOI: 10.1039/x0xx00000x

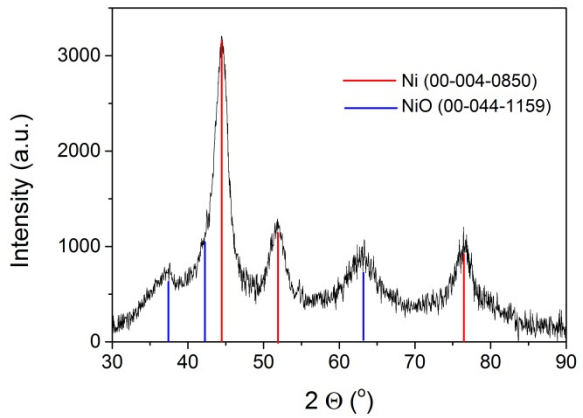

Fig. 1 XRD spectra of the Ni-Al_2O_3/SiO_2 catalyst. Red lines corresponds to Ni metal pattern, and blue lines to NiO pattern.

The commercial Ni-Al_2O_3/SiO_2 sample used as photoresponsive catalyst contains 65% of Ni as determined by inductively coupled plasma-optical emission spectrometry (ICP-OES) analysis. The X-ray diffraction (XRD) revealed that the Ni present in the photocatalyst corresponds mainly to metallic Ni, although NiO was also detected in minor content (Fig. 1). Prior photocatalytic tests the Ni-Al_2O_3/SiO_2 samples have been reduced in H_2 atmosphere at 500 ^{0}C for 2 h. However, XRD of the photocatalyst performed immediately after reduction process showed very similar diffraction pattern to the presented in Fig. 1 (supplementary information Fig. SI1). This is indicating that Ni nanoparticles supported in the aluminium silicate substrate suffers spontaneous oxidation in contact with moisture. The average crystal size of the Ni NPs was estimated to be approximately of 6 nm by Scherrer equation. The average particle size was calculated from a statistically relevant number of measurements from HRTEM images, and it was found of 6.24 ± 1.17 nm. A representative image showing the Ni nanoparticles is presented in the supplementary information as Fig. SI2. These Ni NPs are supported on mixed SiO_2-Al_2O_3 with a Si/Al ratio of 0.23 according to the ICP-OES measurements. The specific surface area, determined by Brunauer-Emmett-Teller (BET) analysis of isothermal gas N_2 adsorption, was of 190 m^2/g. X-ray Photoelectron Spectroscopy (XPS) was performed to the Ni-Al_2O_3/SiO_2 photocatalysts. The XPS Si2p and Al2p spectra were also fitted, obtaining the corresponding components to aluminium silicate at 102.15 eV and 74.17 eV, respectively. Moreover, Si2p peak at 104.86 eV and Al2p peak at 76.54 eV were found, and they are attributed to SiO_2 and Al_2O_3, respectively. The atomic ratio Si/Al was estimated to 0.21, in good agreement with ICP measurement. The core level Ni2p3/2 spectrum with the best deconvolution fit is shown Fig. 2. The Ni2p3/2 curve fitting shows the presence of Ni^0 (857.49 eV) and Ni^{+2} (860.17 eV) in good agreement with previous reports,[18-20] containing a fitting ratio of 30% and 70%, respectively. It is worthy to notice that XPS is a very superficial technique, and the contribution of Ni^0 and Ni^{+2} could be not representative of the whole sample, where core Ni nanoparticle should be constituted by Ni^0 with a NiO shell passivating the nanoparticles.

In a typical reaction 200 mg of the photoresponsive catalyst were compressed at 1 Ton×cm^{-2} for 2 min, and the resulting wafer, crushed and sieved at 0.2 – 0.4 µm, then, loaded on the top of a fritted glass filter inside a cylindrical quartz reactor. The photoreactor can be heated at the required temperature through a heating mantle controlled with a thermocouple.

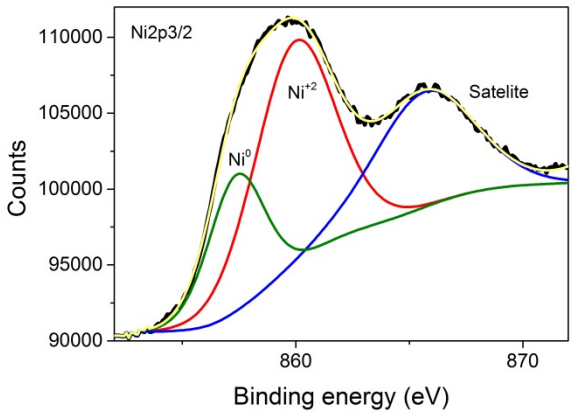

Fig. 2 XPS of Ni 2p spectra of Ni-Al_2O_3/SiO_2 catalyst.

Irradiation was carried out using a UV-Vis 300 W Xe lamp as light source through an optical guide that irradiates the catalyst bed from the top. A photograph of the system is provided in the Supplementary Information (Fig. SI3), in where the photocatalyst can be seen illuminated on top of fritted glass. The gas mixtures containing CO_2 and H_2 diluted in N_2 were introduced from the upper part of the reactor, flowing down through the photocatalyst bed and after leaving the reactor the gas mixture is directly analyzed by an on-line two-column Micro GC instrument allowing to monitor simultaneously CO_2, CO, H_2, CH_4, CH_2-CH_2, CH_3-CH_3 and CH_3-CH_2-CH_3, among others. Quantification was performed by calibrating the response with mixtures of known compositions. Prior to each experiment, the N_2, CO_2 and H_2 flow and temperature of the reactor were equilibrated. Once the system is stabilized, the initial reaction time corresponds to the instant when the light is switched on.

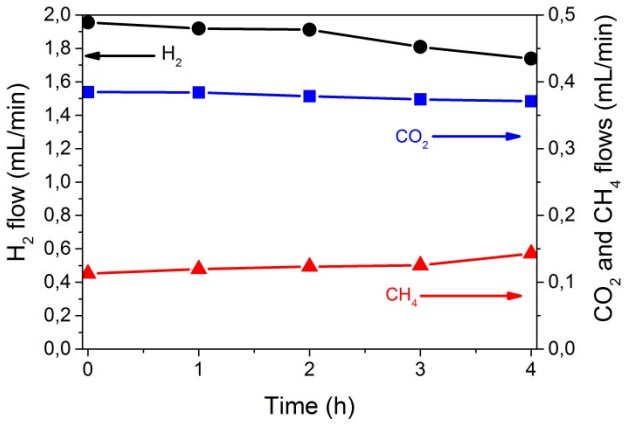

Fig. 3 Flow of CO_2 (blue squares), H_2 (black dots) and CH_4 (red triangles) over time. Reaction conditions: photocatalyst 200 mg, temperature 225 °C, total gas flow 13.9 mL/min with a composition of 81.7% N_2, 3.1 % of CO_2 and 15.2 % of H_2. Light from a 300 w Xe lamp.

Fig. 3 shows individual CO_2, H_2 and CH_4 flows as function of the irradiation time in a typical reaction, using a total flow of 13.9 ml/min. No other products besides CH_4 were detected. Observation of some thermal CH_4 production at 0 time indicates that, at this temperature, under dark conditions CO_2 methanation is already occurring in some extent.

A blank experiment in dark established that at 225 ^{o}C, the thermal methanation takes place at a rate of 50 µL×min^{-1} corresponding to 2 µmol×min^{-1}. Additional control experiments without photocatalyst at 225 ^{0}C in the presence and absence of light irradiation were carried out. However, no detectable amounts of CH_4 were found.

As it can be seen in Fig. 3, the rate of CH_4 formation increases up to a maximum of 143 µL×min^{-1}, corresponding to 5.9 µmol×min^{-1} upon illumination. The temporal variation of the effluent composition is related to the period needed to reach the stationary state concentrations in the system once the light is switched on.

This additional formation of CH_4 by the action of light was accompanied by the corresponding decrease in CO_2 flow rate and the stoichiometric decrease in the H_2 content of the effluent according to Equation 1. Under these conditions about 3.5 % conversion of CO_2 to CH_4 was achieved in the photoassisted process for a contact time of 1.3 s.

The Sabatier reaction (Equation 1) is known to produce H_2O as by-product, which could deactivate the photocatalyst. In order to elucidate the effect of the H_2O adsorption in the Ni-Al_2O_3/SiO_2 photocatalytic tests were carried out passing the reactant gases flow through a bubbler containing H_2O at room temperature and at 50 ^{0}C in order to obtain a relative humidity in the initial gases flow of approximately 20 and 40 %, respectively. As can be observed in Fig SI4 in the supplementary information the addition of 20 % relative humidity produced a 32% reduction in the CH_4 production. Further increase in the relative humidity in the steam (40%) resulted in a 38% lower CH_4 evolution. This is indicating that at these reaction conditions (225 ^{o}C with a reagents gas flow 13.9 mL/min with a composition of 81.7% N_2, 3.1 % of CO_2 and 15.2 % of H_2) the introduction of H_2O produced a detrimental effect in the photoassisted CH_4 production. However, the reduction of CH_4 flow was lower than 40% was relative humidity up to 40 % was introduced probably due to the employed temperature of 225 ^{0}C, which induce H_2O desorption, and the continuous flow operation mode, which contributes to the elimination of the desorbed by-product from the photocatalyst bed.

The influence of the light intensity and the wavelength in the photoassisted methanation of CO_2 at constant 225 ^{o}C is presented in Fig. 4. As it can be seen there, CO_2 methanation already occurs in some extent in the dark at 225 ^{o}C resulting in constant formation of 15 µL/min of CH_4 along time when a total flow of 14.28 mL/min was employed (composed by 11.39 mL×min^{-1} of H_2 and 2.85 mL×min^{-1} of CO_2).

At full illumination (Light 100% plot in Fig. 4), a fast increase in CH_4 production was monitored due to irradiation, reaching a stationary value of 55 µL/min.

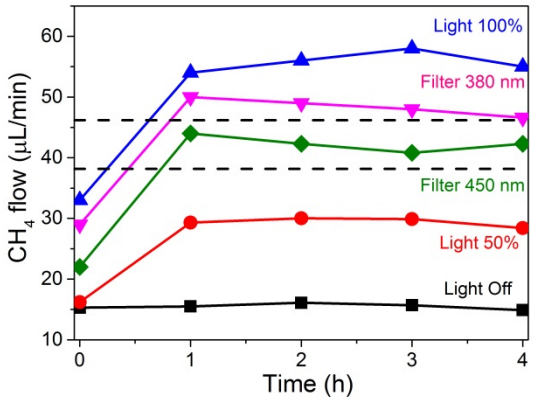

Fig. 4 Flow of CH_4 at 225 ^{o}C under different illumination conditions. Light 100% corresponds to 2327 W/m^2 irradiance and light 50 % to 1163 W/m^2. Filter 380 nm and 450 nm correspond, respectively, to full illumination at 2327 W/m^2 using cut-off filters for wavelengths shorter than 380 nm or 450 nm, respectively. Light Off corresponds to dark conditions. Reaction conditions: photocatalyst 200 mg, total gas flow of 14.28 mL×min^{-1} composed by 11.39 mL×min^{-1} of H_2 and 2.85 mL×min^{-1} of CO_2. The dotted straight lines indicate the theoretical CH_4 formation rate considering the reduction in the light intensity due to the cut-off part of the lamp power.

This means that, under these conditions of flow, composition, temperature and light power, light increased CH_4 production by a factor of 3.7 times, reaching CO_2 conversions close to 2 %. Note that this conversion is lower than reported in the previous experiment in Fig. 3. This is due to the higher reactants concentration employed in this experiment (no N_2 dilution) and the higher total gas flux. At half power illumination (Light 50% plot), obtained with a neutral filter with optical density of 50%, this fast initial rate was observed as well, and a CH_4 flux of 30 µL/min, approximately half the value obtained with full illumination, was measured. This experiment confirms again that light is responsible for the formation of CH_4, whose concentration decreases proportionally as the light intensity decreases.

The influence of the irradiation wavelength was addressed by using cut-off filters. Since the intensity of the xenon lamp is approximately constant at all wavelengths in the range between 300 and 800 nm (see Fig. SI5 in Supporting Information), cutting a range of wavelengths in the UV region decreases proportionally the intensity of the light transmitted through the filter. Therefore, the cut-off filters not only removes shorter wavelengths, but also decreases the light flux reaching the photoresponsive catalyst (about 84 and 70% for cut-off filters of 380 and 450 nm, respectively). The results of the photoresponse of the Ni-Al_2O_3/SiO_2 catalyst are also presented in Fig. 4. As it can be seen there, cut-off filters for wavelengths shorter than 380 or 450 nm, removing partially or totally the UV component from the xenon lamp, leads to some decrease in CH_4 formation rate in accordance with the expected proportion of light power decreased by the filter (see Fig. 3). Importantly, Fig. 4 clearly shows that a notable CH_4 production is still observed in the absence of UV light, indicating that the photoresponse of the catalyst has an important contribution of the visible light zone of the spectrum (about 70%). This photoresponse is in agreement

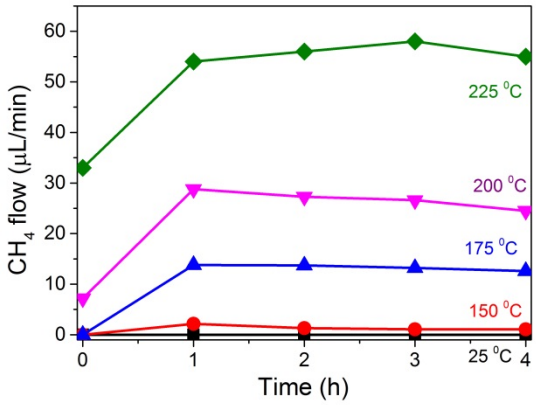

Fig. 5 Influence of the reaction temperature on CH_4 evolution under illumination at 240 mW/cm^2 power under continuous flow. Photocatalyst (200 mg) as powder obtained by compressing and sieving as 0.2 – 0.4 µm pellets. A total gas flow of 22.23 ml/ min was introduced in the reactor containing 17.82 and 4.41 ml/min of H_2 and CO_2, respectively.

with the diffuse-reflectance UV-Vis spectrum of the photocatalyst presented in Fig. SI6 that shows a continuous absorption in the whole UV and visible regions, increasing the absorption intensity toward the shorter wavelength zone of the spectrum. Thus, it can be concluded that the photoresponse follows the absorption spectrum of Ni NPs in the Ni-Al_2O_3/SiO_2 catalyst. It is worthy noticing that in all experiments the reactor temperature is continuously monitored and controlled by a thermopar coupled to a heating mantle and a controller, avoiding temperature changes upon light intensity variations.

The temperature dependence of this photoassisted continuous flow methanation was studied in the range from ambient to 225 °C. The results are presented in Fig. 5. As indicated above, the temporal increase in the CH_4 formation rate reflects the time to reach the steady state regime in the photoreactor at the flow of the experiment. As it can be observed there, negligible amount of CH_4 was detected at room temperature either in the dark or under illumination. However, as soon as the temperature was increased from 150 °C up to 225 °C, the photoassisted CH_4 production was observed. This temperature dependence is not surprising and it has been reported previously for this photoassisted reaction under batch mode. [17] Worth noting is that the thermal, dark process of CH_4 formation under our experimental conditions starts to be detected above 175 °C. Therefore, in comparison with the production plots shown in Figure 1 and 2, no thermal CH_4 is observed in the dark at 175 °C, while under Xe lamp irradiation a CH_4 formation rate of 14 µL×min^{-1} was measured. From the CH_4 formation rates measured at different temperatures, an apparent activation energy of 45.9 kJ×mol^{-1} was calculated for this reaction, using Ni-Al_2O_3/SiO_2 as catalyst, which is consistent with activation energies previously reported using other Ni-based catalysts. [21]

For comparison purposes, CO_2 methanation reaction at 150 °C was also performed in batch using the same Ni-Al_2O_3/SiO_2 photocatalyst. Note that at this temperature no CH_4 is formed in the dark. A CH_4 formation rate of 16.67 µmol×min^{-1} was measured in batch using the same amount of catalysts (200 mg). This CH_4 formation rate value is similar to that previously reported. [17] In the present case, under continuous flow at 150 °C, a CH_4 formation rate of 2 µL×min^{-1} has been measured. If only the contribution of light to the formation of CH_4 is considered, an apparent value of quantum efficiency, i.e. mols of CH_4 formed divided by mols of photons, from both batch and continuous flow procedures can be estimated. It was determined that the apparent quantum yield of CH_4 formation for both the batch and the continuous flow processes were coincident, obtaining a number of 0.11 molecules of CH_4 per photon.

This coincidence indicates that the efficiency of this photoassisted reaction is independent from the operation mode, as it should be for a common reaction mechanism. According to the current proposals, it is suggested that light absorption by Ni NPs must increase their instantaneous local temperature measured at the nanometric scale and this localized photothermal effect results in an acceleration of the reaction rate.

On the other hand, it has been reported in batch conditions that besides CH_4, low but detectable amounts of CO are formed in the process. [17] However, in the present case under continuous flow, the only detectable product was CH_4 and CO was below the detection limit (0.2 µl×min^{-1}) Thus, selectivity is enhanced under flow conditions, probably due to the limited CO_2 conversion value.

In conclusion, the present study shows that the efficiency of methanation of CO_2 by H_2 is sufficiently high to allow performing the process under continuous flow operation, reaching substantial CO_2 conversions, even for very short CO_2-catalyst contact times. Depending on the reactor temperature, illumination in the UV or visible region of commercial Ni-Al_2O_3/SiO_2 catalysts promotes methanation or increases CH_4 formation rate respect to the same process in the dark, up to 3.7 times at 225 °C and conversions about 3.5 % can be reached. The system does not undergo apparent deactivation in 4 h reaction time. Comparison between batch and continuous modes illustrates that although the quantum efficiency is almost coincident in both operation modes, the overall CH_4 production is higher in continuous systems. On the other hand, the selectivity is improved in continuous mode, where formation of CO is not detected.

Acknowledgements

Financial support by the Spanish Ministry of Economy and Competitiveness (Severo Ochoa and CTQ2015-65169-CO2-R1) is gratefully acknowledged. J.A. thanks the Universitat Politécnica de Valencia for post-doctoral research associate contract.

Notes and references

1. A. J. Nozik and J. Miller, *Chemical Reviews*, 2010, **110**, 6443-6445.

2. H. Arakawa, M. Aresta, J. N. Armor, M. A. Barteau, E. J. Beckman, A. T. Bell, J. E. Bercaw, C. Creutz, E. Dinjus, D. A. Dixon, K. Domen, D. L. DuBois, J. Eckert, E. Fujita, D. H. Gibson, W. A. Goddard, D. W. Goodman, J. Keller, G. J. Kubas, H. H. Kung, J. E. Lyons, L. E. Manzer, T. J. Marks, K. Morokuma, K. M. Nicholas, R. Periana, L. Que, J. Rostrup-Nielson, W. M. H. Sachtler, L. D. Schmidt, A. Sen, G. A. Somorjai, P. C. Stair, B. R. Stults and W. Tumas, *Chemical Reviews*, 2001, **101**, 953-996.
3. K. Li, X. An, K. H. Park, M. Khraisheh and J. Tang, *Catalysis Today*, 2014, **224**, 3-12.
4. S. Rönsch, J. Schneider, S. Matthischke, M. Schlüter, M. Götz, J. Lefebvre, P. Prabhakaran and S. Bajohr, *Fuel*, 2016, **166**, 276-296.
5. S. K. Hoekman, A. Broch, C. Robbins and R. Purcell, *International Journal of Greenhouse Gas Control*, 2010, **4**, 44-50.
6. P.-W. Pan and Y.-W. Chen, *Catalysis Communications*, 2007, **8**, 1546-1549.
7. F. Sastre, A. V. Puga, L. Liu, A. Corma and H. García, *Journal of the American Chemical Society*, 2014, **136**, 6798-6801.
8. Ș. Neațu, J. Maciá-Agulló and H. Garcia, *International Journal of Molecular Sciences*, 2014, **15**, 5246.
9. Y. Zhao, G. Chen, T. Bian, C. Zhou, G. I. N. Waterhouse, L.-Z. Wu, C.-H. Tung, L. J. Smith, D. O'Hare and T. Zhang, *Advanced Materials*, 2015, **27**, 7824-7831.
10. O. K. Varghese, M. Paulose, T. J. LaTempa and C. A. Grimes, *Nano Letters*, 2009, **9**, 731-737.
11. X. Meng, T. Wang, L. Liu, S. Ouyang, P. Li, H. Hu, T. Kako, H. Iwai, A. Tanaka and J. Ye, *Angewandte Chemie*, 2014, **126**, 11662-11666.
12. J. Jia, P. G. O'Brien, L. He, Q. Qiao, T. Fei, L. M. Reyes, T. E. Burrow, Y. Dong, K. Liao, M. Varela, S. J. Pennycook, M. Hmadeh, A. S. Helmy, N. P. Kherani, D. D. Perovic and G. A. Ozin, *Advanced Science*, 2016, **3**, n/a-n/a.
13. J. Ren, S. Ouyang, H. Xu, X. Meng, T. Wang, D. Wang and J. Ye, *Advanced Energy Materials*, 2017, **7**, n/a-n/a.
14. I. Kocemba, J. Nadajczyk, J. Góralski and M. I. Szynkowska, *Polish Journal of Chemical Technology*, 2010, **12**, 1-2.
15. K. Gilmore and P. H. Seeberger, *The Chemical Record*, 2014, **14**, 410-418.
16. S. Sicardi, G. Baldi, L. van Dierendonck and T. Smeets, *Chemical Engineering Science*, 1988, **43**, 1843-1848.
17. J. Albero, H. Garcia and A. Corma, *Topics in Catalysis*, 2016, **59**, 787-791.
18. T.-Y. Yung, L.-Y. Huang, T.-Y. Chan, K.-S. Wang, T.-Y. Liu, P.-T. Chen, C.-Y. Chao and L.-K. Liu, *Nanoscale Research Letters*, 2014, **9**, 444.
19. S. Kasztelan, J. Grimblot, J. P. Bonnelle, E. Payen, H. Toulhoat and Y. Jacquin, *Applied Catalysis*, 1983, **7**, 91-112.
20. A. M. Venezia, R. Bertoncello and G. Deganello, *Surface and Interface Analysis*, 1995, **23**, 239-247.
21. Y. Feng, W. Yang and W. Chu, *International Journal of Chemical Engineering*, 2015, **2015**, 7.